J|A|C|S
ARTICLES
Published on Web 04/27/2006

On the Origin of the Stereoselectivity in the Alkylation of Oxazolopiperidone Enolates

Ignacio Soteras,[†] Oscar Lozano,[‡] Arantxa Gómez-Esqué,[‡] Carmen Escolano,[‡] Modesto Orozco,[§,⊥] Mercedes Amat,[‡] Joan Bosch,*[,‡] and F. Javier Luque*[,†]

Contribution from the Department of Physical Chemistry, Faculty of Pharmacy, University of Barcelona, Av. Diagonal 643, 08028 Barcelona, Spain, Laboratory of Organic Chemistry, Faculty of Pharmacy, University of Barcelona, Av. Joan XXIII s/n, 08028 Barcelona, Spain, and Molecular Modeling and Bioinformatics Unit, Scientific Park of Barcelona, Josep Samitier 1-6, 08028 Barcelona, Spain

Received August 25, 2005; E-mail: fjluque@ub.edu; joanbosch@ub.edu

Abstract: The origin of the diastereoselective alkylation of enolates of oxazolopiperidones is studied by means of theoretical calculations and experimental assays. For the unsubstituted oxazolopiperidone, the alkylation with methyl chloride is predicted to afford mainly the *exo* product, a finding further corroborated from the analysis of the experimental outcome obtained in the reaction of the racemic oxazolopiperidone. However, such a preference can be drastically altered by the presence of substituents attached to the fused ring. In particular, when the angular carbon adopts an *R* configuration in a phenylglycinol-derived oxazolopiperidone, the presence of a phenyl ring at position 3 forces the *pseudo*-planarity of the bicyclic lactam, and the diastereoselectivity is dictated by the internal torsional strain induced in the enolate. However, when the angular carbon adopts an *S* configuration, the preference for the *exo* alkylation stems from the intermolecular steric hindrance between the enolate and the alkylating reagent. Interestingly, the intramolecular hydrogen bond formed between the phenyl ring and the carbonyl oxygen in the enolate largely reduces the difference in stability of the two TSs compared to the unsubstituted oxazolopiperidone.

Introduction

The origin of the π-facial stereoselectivity in reactions leading to carbon−carbon bond formation through enolate alkylation is a controversial topic in organic synthesis.[1] Meyers and co-workers noticed an impressive *endo* selectivity in the alkylation of the enolate carbon in bicyclo[3.3.0]lactams **1**, where the ratio between *endo* and *exo* products was found to be 10−50:1 (see Scheme 1).[2] However, the *endo*:*exo* diastereofacial selectivity in structurally related bicyclic lactams has proven to be largely dependent on both the nature of the fused ring and the presence of substituents.[3] For instance, alkylation of the enolates derived from **2** and **3** preferentially leads to the *exo* product. The finding that highly selective alkylation still occurs even from monocyclic lactam enolates **4**−**6** suggests that factors other than steric considerations related to the concave−convex faces of the enolate can play a relevant role.[4]

Scheme 1

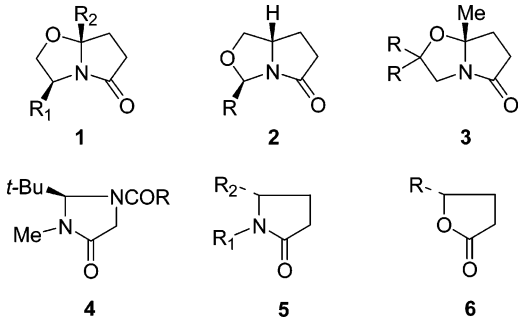

1 **2** **3** **4** **5** **6**

For the enolate of imidazolidinone **4**, Seebach et al. suggested the involvement of stereoelectronic effects based on a slight pyramidalization of the enolate β-carbon.[4b] On the other hand, Meyers and co-workers[5] related the diastereofacial selectivity in **5** to the preference for an electrophilic attack anti to the nitrogen lone pair. The competition between this latter effect

[†] Department of Physical Chemistry, Faculty of Pharmacy, University of Barcelona.
[‡] Laboratory of Organic Chemistry, Faculty of Pharmacy, University of Barcelona.
[§] Molecular Modeling and Bioinformatics Unit, Scientific Park of Barcelona.
[⊥] Computational Biology Program, Barcelona Supercomputing Center, Jordi Girona 31, Edifici Torre Girona, Barcelona 08028, Spain.

(1) Högberg, H.-E. In *Stereoselective Synthesis, Methods of Organic Chemistry* (*Houben-Weyl*); Helmchen, G., Hoffmann, R. W., Mulzer, J., Schaumann, E., Eds.; Thieme: Stuttgart, 1996; E21, Vol. 2, pp 794−915.
(2) For reviews, see: (a) Romo, D.; Meyers, A. I. *Tetrahedron* **1991**, *47*, 9503. (b) Meyers, A. I.; Brengel, G. P. *Chem. Commun.* **1997**, 1. (c) Groaning, M. D.; Meyers, A. I. *Tetrahedron* **2000**, *56*, 9843.
(3) (a) Roth, G. P.; Leonard, S. F.; Tong, L. *J. Org. Chem.* **1996**, *61*, 5710. (b) Meyers, A. I.; Seefeld, M. A.; Lefker, B. A. *J. Org. Chem.* **1996**, *61*, 5712. (c) Bailey, J. H.; Byfield, A. T. J.; Davis, P. J.; Foster, A. C.; Leech, M.; Moloney, M. G.; Müller, M.; Prout, C. K. *J. Chem. Soc., Perkin Trans. 1* **2000**, 1977 and references therein.
(4) (a) Tomioka, K.; Cho, Y.-S.; Sato, F.; Koga, K. *J. Org. Chem.* **1988**, *53*, 4094. (b) Seebach, D.; Maetzke, T.; Petter, W.; Klötzer, B.; Plattner, D. A. *J. Am. Chem. Soc.* **1991**, *113*, 1781. (c) Ezquerra, J.; Pedregal, C.; Rubio, A.; Yruretagoyena, B.; Escribano, A.; Sánchez-Ferrando, F. *Tetrahedron* **1993**, *49*, 8665. (d) Breña-Valle, L. J.; Carreón, R.; Cruz-Almanza, R. *Tetrahedron: Asymmetry* **1996**, *7*, 1019. (e) Charrier, J.-D.; Duffy, J. E. S.; Hitchcock, P. B.; Young, D. W. *Tetrahedron Lett.* **1998**, *39*, 2199. (f) Maldaner, A. O.; Pilli, R. A. *Tetrahedron* **1999**, *55*, 13321.

and steric factors was later used to rationalize the diastereofacial selectivity in other bicyclic lactams.[6] In contrast to the preceding studies, chelation of the enolate by the metal (lithium) ion has been considered to be the origin of the diastereofacial selectivity in **5**.[7] Houk and co-workers, however, have rationalized the stereochemistry in the enolate alkylation of **5** from the torsional strain in the transition state,[8] which has recently received further support from the analysis of the stereoselective alkylation of 4-substituted γ-butyrolactones **6**.[9]

The diastereoselective alkylation of chiral nonracemic oxazolopiperidones has been used as the key step in the enantioselective synthesis of a variety of building blocks and natural products.[10] In particular, we have shown that the enolates of the bicyclic lactams **7**, after treatment with several alkylating reagents, afforded mixtures of two separable diastereomers with a high stereoselectivity for the *exo* products **8** (see Scheme 2). In contrast, the alkylation reaction of **10** yielded mixtures of *endo* and *exo* products, where the former were the major products.

The aim of this study is to explore the origin of the stereoselectivity in the alkylation of the enolates derived from oxazolopiperidones **7** and **10**, which to the best of our knowledge is the first theoretical analysis performed for six-membered ring lactams. To this end, we first examine the energetic features in the alkylation of the enolate formed from the unsubstituted oxazolopiperidone **13**, which are subsequently used to explore the influence played by the phenyl substituent in the stereochemical outcome obtained for derivatives **7** and **10**. The results are used to discuss the factors that modulate the stereoselective alkylation in these compounds and to design chemical modifications that might be used to tune the diastereoselective alkylation in related substituted oxazolopiperidones.

Scheme 2

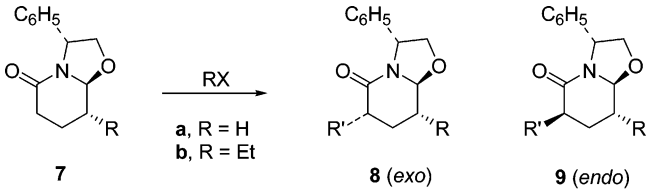

7 8 (*exo*) 9 (*endo*)

R	R_1	X	*exo*/*endo*	Ref.
H	Et	I	100:0	10e
H	Me	I	85:15	10k
H	Bn	Br	77:23	10k
Et	Me	I	95:5	10i
Et	CH_2CO_2tBu	Br	77:23	10i

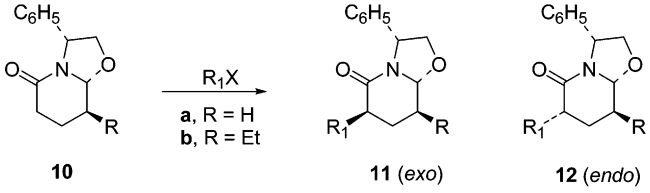

10 11 (*exo*) 12 (*endo*)

R	R_1	X	*exo*/*endo*	Ref.
H	Et	I	32:68	10k
Et	Me	I	24:76	10i
Et	CH_2CO_2tBu	Br	12:88	10i

Methods

Computational Details. Full geometry optimizations were performed with the B3LYP[11] density functional method using the 6-31+G(d) basis set. The nature of the stationary points was verified by inspection of the vibrational frequencies within the harmonic oscillator approximation. Intrinsic reaction coordinate calculations[12] were carried out to check the connection between the transition states and the minimum energy structures. Single-point MP2/6-31+G(d) and MP2/aug-cc-pVDZ calculations were subsequently performed to determine the relative energies of the different species formed in the alkylation process. The suitability of this computational scheme has been recently supported from the results determined at different levels of theory for the S_N2 reaction of lithium enolate of acetaldehyde with chloromethane, which showed that the energetic features determined from single-point MP2 calculations on B3LYP geometries were in close agreement to those obtained from full MP2 geometry optimizations.[13] This strategy is also supported by previous studies of S_N2 reactions where the geometries predicted at the B3LYP level are similar to those obtained from MP2 calculations.[14] Finally, it can be expected that the electronic influence played by the chemical environment in the enolate of oxazolopiperidone will be captured from calculations at the B3LYP level,[15] which indeed will benefit from the expected cancellation of inaccuracies in the comparison of the relative stability of the transition states (and products) formed along the *endo* and *exo* alkylation reactions. For the unsubstituted oxazolopiperidone the contribution of higher-order electron correlation effects was estimated from CCSD/6-31+G(d) calculations. Our best estimate of the energy difference between the stationary points was then determined by combining the relative energies computed at the MP2/aug-cc-pVDZ level and the difference between the energies obtained from CCSD and MP2 calculations performed with the 6-31+G(d) basis set. Zero-point, thermal, and entropic corrections evaluated within the framework of the harmonic oscillator-rigid rotor

(5) Meyers, A. I.; Seefeld, M. A.; Lefker, B. A.; Blake, J. F. *J. Am. Chem. Soc.* **1997**, *119*, 4565.
(6) Meyers, A. I.; Seefeld, M. A.; Lefker, B. A.; Blake, J. F.; Williard, P. G. *J. Am. Chem. Soc.* **1998**, *120*, 7429.
(7) (a) Ikuta, Y.; Tomoda, S. *Tetrahedron Lett.* **2003**, *44*, 5931. (b) Ikuta, Y.; Tomoda, S. *Org. Lett.* **2004**, *6*, 189.
(8) Ando, K.; Green, N. S.; Li, Y.; Houk, K. N. *J. Am. Chem. Soc.* **1999**, *121*, 5334.
(9) Ando, K. *J. Am. Chem. Soc.* **2005**, *127*, 3964.
(10) (a) Meyers, A. I.; Hanreich, R.; Wanner, K. T. *J. Am. Chem. Soc.* **1985**, *107*, 7776. (b) Meyers, A. I.; Lefker, B. A.; Wanner, K. T.; Aitken, R. A. *J. Org. Chem.* **1986**, *51*, 1936. (c) Meyers, A. I.; Berney, D. *J. Org. Chem.* **1989**, *54*, 4673. (d) Resek, J. E.; Meyers, A. I. *Synlett* **1995**, 145. (e) Amat, M.; Pshenichnyi, G.; Bosch, J.; Molins, E.; Miravitlles, C. *Tetrahedron: Asymmetry* **1996**, *7*, 3091. (f) Schwarz, J. B.; Meyers, A. I. *J. Org. Chem.* **1998**, *63*, 1619. (g) Reeder, M. R.; Meyers, A. I. *Tetrahedron Lett.* **1999**, *40*, 3115. (h) Hughes, R. C.; Dvorak, C. A.; Meyers, A. I. *J. Org. Chem.* **2001**, *66*, 5545. (i) Amat, M.; Escolano, C.; Lozano, O.; Llor, N.; Bosch, J. *Org. Lett.* **2003**, *5*, 3139. (j) Brewster, A. G.; Broady, Davies, D. E.; Heightman, T. D.; Hermitage, S. A.; Hughes, M.; Moloney, M. G.; Woods, G. *Org. Biomol. Chem.* **2004**, *2*, 1031. (k) Amat, M.; Escolano, C.; Llor, N.; Lozano, O.; Gómez-Esqué, A.; Griera, R.; Bosch, J. *Arkivoc* **2005**, 115.
(11) (a) Becke, A. B. *J. Chem. Phys.* **1993**, *98*, 5648. (b) Becke, A. B. *Phys. Rev. A* **1998**, *38*, 3098. (c) Lee, C.; Yang, W.; Parr, R. G. *Phys. Rev. B* **1988**, *37*, 785.
(12) (a) Gonzalez, C.; Schlegel, H. B. *J. Chem. Phys.* **1989**, *90*, 2154. (b) Gonzalez, C.; Schlegel, H. B. *J. Phys. Chem.* **1990**, *84*, 5523.
(13) Pratt, L. M.; Van Nguyen, N.; Ramachandran, B. *J. Org. Chem.* **2005**, *70*, 4279.
(14) Glukhovtsev, M. N.; Bach, R. D.; Pross, A.; Radom, L. *Chem. Phys. Lett.* **1996**, *260*, 558.
(15) (a) Soliva, R.; Orozco, M.; Luque, F. J. *J. Comput. Chem.* **1997**, *18*, 980. (b) De Proft, F.; Martin, J. M. L.; Geerlings, P. *Chem. Phys. Lett.* **1996**, *250*, 393.

Scheme 3

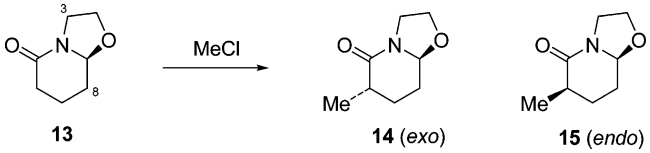

13 **14** (*exo*) **15** (*endo*)

at 1 atm and 298 K were added to the electronic energies to estimate the free energy differences in the gas phase.

To estimate the influence of solvation, QM SCRF continuum calculations were performed by using the B3LYP/6-31G(d) optimized version of the MST(IEF) model,[16] which relies on the Integral Equation formalism (IEF)[17] of the polarizable continuum model.[18] Since the MST model has not been parametrized to treat solvation in tetrahydrofuran (i.e., the solvent used in experimental assays), calculations were performed for the solvation in water, octanol, chloroform, and carbon tetrachloride in order to explore the effect of varying the polarity of the solvent.[16,19] Following the standard procedure in the MST model, the free energy of solvation was computed by using the gas-phase optimized geometries.[20] The relative stability in solution was estimated by combining the free energy difference in the gas phase and the differences in free energy of solvation determined from MST calculations.[21]

Gas-phase calculations were carried out using Gaussian-03.[22] MST calculations were performed using a locally modified version of Gaussian-03.[23]

Experimental Procedures. All the reactions were carried out generating the enolate of lactams **7**, **10**, and **13** at low temperature (−78 °C) during 1 h using lithium bis(trimethylsilyl)amide (1 M in THF, 1.5 equiv) as the base, followed by addition of the alkylating reagent (2.5 equiv). The reaction mixture was then stirred at −78 °C during 2 h and quenched by addition of a saturated aqueous solution of sodium chloride. Reactions were performed using THF as the solvent.

Results and Discussion

Intrinsic Stereoselective Alkylation of the Oxazolopiperidone Enolate. The intrinsic stereofacial selectivity in the alkylation of the oxazolopiperidone enolate was examined by considering the reaction of the enolate derived from the unsubstituted oxazolopiperidone **13** with methyl chloride (see Scheme 3). The results (see Table 1) point out that the compound resulting from an *exo* alkylation (**14**) is favored by near 1 kcal/mol with regard to the *endo* product (**15**). Moreover, by combining gas phase results with solvation free energies, such a difference is predicted to remain essentially unaffected irrespective of the polarity of the solvent.

Table 1. Energy (Corrected for Zero-Point Energy; ZPE)[a] and Free Energy Differences (at 298 K; kcal/mol)[a] of Separated Products Formed in the Reaction of the Enolate Derived from the Unsubstituted Oxazolopiperidone **13** with Methyl Chloride with Regard to Separated Reactants in the Gas Phase and in Solution

	gas		CCl_4	$CHCl_3$	octanol	water
product	$\Delta(E+\text{ZPE})$	ΔG	ΔG	ΔG	ΔG	ΔG
			MP2/6-31+G(d)			
14 (*exo*)	−51.8	−47.4	−51.5	−54.0	−55.3	−58.1
15 (*endo*)	−51.0	−46.4	−50.5	−53.1	−54.4	−57.2
Δ^b	0.8	1.0	1.0	0.9	0.9	1.0
			MP2/aug-cc-pVDZ			
14 (*exo*)	−53.4	−49.0	−53.1	−55.6	−56.9	−59.7
15 (*endo*)	−52.7	−48.2	−52.2	−54.8	−56.1	−58.8
Δ^b	0.7	0.8	0.9	0.8	0.8	0.9
			Best Estimate[c]			
14 (*exo*)	−54.7	−50.2	−54.4	−56.9	−58.2	−61.0
15 (*endo*)	−53.9	−49.3	−53.4	−56.0	−57.3	−60.0
Δ^b	0.8	0.9	1.0	0.9	0.9	1.0

[a] Values determined by subtracting the (free) energy of reactants (enolate of **13** and methyl chloride) from the (free) energy of products (**14** or **15** and chloride anion). [b] *Endo* − *Exo*. [c] Values determined from MP2/aug-cc-pVDZ+[CCSD-MP2/6-31+G(d)] calculations.

To verify experimentally the preference of the oxazolopiperidone enolate for the *exo* alkylation, we determined the *exo*:*endo* ratio in the product mixtures obtained after the alkylation of the racemic enolate derived from **13** with methyl iodide. The *exo*:*endo* ratio was 80:20,[24] which implies a free energy difference of 0.5 kcal/mol at the temperature (−78 °C) used under experimental conditions. A similar ratio (75:25) was obtained when the reaction was carried out in the presence of HMPA.

The potential influence of kinetic effects in the stereoselective alkylation of the enolate of **13** was explored by determining the relative energy of the transition states (as well as the prereaction and postreaction complexes) for the *endo*/*exo* alkylation with methyl chloride. The prereaction complexes leading to *endo* and *exo* products have similar stabilities. The distance from the carbon atom in methyl chloride (denoted C_M hereafter) to the carbon atom (C_α) vicinal to the carbonyl group in the enolate was similar in the two complexes (∼3.54 Å in the *endo* and *exo* complexes). Moreover, a C−H···O interaction between the carbonyl oxygen and one of the hydrogen atoms in methyl chloride (O···H(C_M) distances of ∼2.12 Å in *endo* and *exo* complexes) was identified. Such an interaction was confirmed by the existence of a bond path between O and H atoms,[25] whose electron density at the bond critical point (ρ_{bcp}∼0.0200 au in both *endo* and *exo* species) lies within the range of values reported for similar interactions.[26] In contrast to the results obtained for the prereaction complexes, the TS for the *endo* attack is destabilized relative to the *exo* TS by 1.7 kcal/mol at the MP2/6-31+G(d) and MP2/aug-cc-pVDZ levels and by 1.4 kcal/mol according to our best estimate obtained after inclusion of higher-order electron correlation effects (see Figure 1).[27] The different stability of the two transition states is also reflected in the C_α−C_M distance, which is 0.031 Å shorter

(16) (a) Bachs, M.; Luque, F. J.; Orozco, M. *J. Comput. Chem.* **1994**, *15*, 446. (b) Curutchet, C.; Orozco, M.; Luque, F. J. *J. Comput. Chem.* **2001**, *22*, 1180. (c) Soteras, I.; Curutchet, C.; Bidon-Chanal, A.; Orozco, M.; Luque, F. J. *THEOCHEM* **2005**, *727*, 29.
(17) (a) Cancès, E.; Mennucci, B. *J. Math. Chem.* **1998**, *23*, 309. (b) Cancès, E.; Mennucci, B.; Tomasi, J. *J. Chem. Phys.* **1997**, *107*, 3032. (c) Mennucci, B.; Cancès, E.; Tomasi, J. *J. Phys. Chem. B* **1997**, *101*, 10506.
(18) (a) Miertus, S.; Scrocco, E.; Tomasi, J. *Chem. Phys.* **1981**, *55*, 117. (b) Miertus, S.; Tomasi, J. *Chem. Phys.* **1982**, *65*, 239.
(19) (a) Orozco, M.; Bachs, M.; Luque, F. J. *J. Comput. Chem.* **1995**, *16*, 563. (c) Luque, F. J.; Zhang, Y.; Aleman, C.; Bachs, M.; Gao, J.; Orozco, M. *J. Phys. Chem.* **1996**, *100*, 4269. (d) Luque, F. J.; Alemán, C.; Bachs, M.; Orozco, M. *J. Comput. Chem.* **1996**, *17*, 806.
(20) Luque, F. J.; López-Bes, J. M.; Cemeli, J.; Aróztegui, M.; Orozco, M. *Theor. Chem. Acc.* **1997**, *96*, 105.
(21) Since the MST model was parametrized from experimental free energies of solvation at 298 K, the gas-phase free energy difference was also determined at this temperature for the sake of internal consistency.
(22) Frisch, M. J. et al. *Gaussian 03*, revision B.04; Gaussian, Inc.: Pittsburgh, PA, 2003.
(23) Peterson, M.; Poirier, R. Monster Gauss; Department of Biochemistry, University of Toronto, Canada. Version modified by Cammi, R.; Tomasi, J. (1987) and by Curutchet, C.; Orozco, M.; Luque, F. J. (2003).
(24) NMR was used to determine the stereochemistry of the alkylated derivatives, taking advantage of the γ-gauche shielding effect upon C8 when the substituent at C6 adopts a pseudoaxial disposition.
(25) Bader, R. F. W. *Chem. Rev.* **1991**, *91*, 893.
(26) (a) Kock, U.; Popelier, P. L. A. *J. Phys. Chem.* **1995**, *99*, 9747. (b) Popelier, P. L. A. *J. Phys. Chem. A* **1998**, *102*, 1873. (c) Cubero, E.; Orozco, M.; Hobza, P.; Luque, F. J. *J. Phys. Chem. A* **1999**, *103*, 6394−6401.

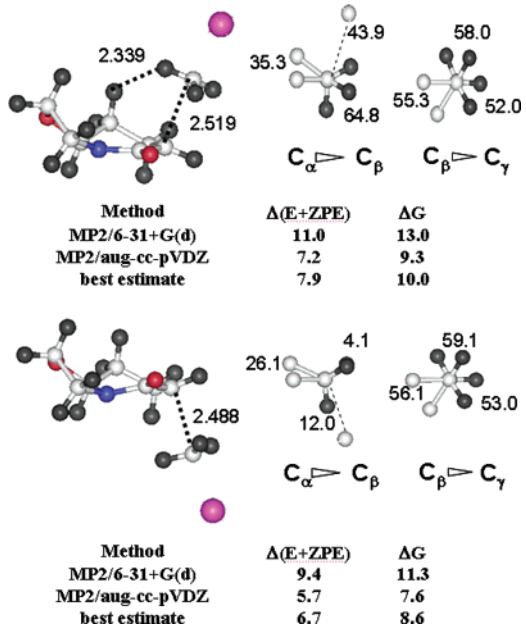

Figure 1. Transition structures for the *endo* (top) and *exo* (bottom) addition of methyl chloride to the enolate of oxazolopiperidone **13**. Energies (corrected for zero-point energy; ZPE) and free energies (at 298 K; kcal/mol) determined at the MP2/6-31+G(d) and MP2/aug-cc-pVDZ levels and the best estimate [MP2/aug-cc-pVDZ+(CCSD-MP2)/6-31+G(d)] relative to the most stable prereaction complex are also shown, together with the Newman projections viewed from the directions along the $C_\alpha-C_\beta$ and $C_\beta-C_\gamma$ bonds.

in the *exo* TS (2.488 Å) than in the *endo* TS (2.519 Å). Finally, the postreaction complex formed through the *exo* addition is around 5 kcal/mol more stable than that obtained in the *endo* attack.

The Newman projection for the bond between enolate carbon atoms C_α and C_β and between C_β and C_γ is also shown in Figure 1. While there is no relevant difference in the arrangement along the $C_\beta-C_\gamma$ bond in the two TSs, the *exo* TS occurs with a more eclipsed arrangement than the *endo* TS along the $C_\alpha-C_\beta$ bond, which would be in opposition to the greater stability of the *exo* TS. Nevertheless, the approach of the incoming methyl group in the *endo* TS is sterically impeded by the repulsive contact with the axial hydrogen at the enolate Cγ atom (H···H distance of 2.339 Å; see Figure 1), which is shorter than the sum of van der Waals radii (2.4 Å). In contrast, a similar steric hindrance was not observed for the approach of methyl chloride in the *exo* TS.

To verify the preceding findings, the geometries of the *endo* and *exo* transition states were fully optimized at the MP2/6-31+G(d) level. Though the length of the forming $C_\alpha-C_M$ bonds in the transition states are somewhat smaller compared to the B3LYP/6-31+G(d) values, the $C_\alpha-C_M$ bond length in the *exo* TS (2.306 Å) is 0.033 Å shorter than that in the *endo* TS (2.339 Å), which agrees with the geometrical difference found from B3LYP/6-31+G(d) geometry optimizations (0.031 Å). Moreover, the TS for the *endo* attack is destabilized relative to the *exo* TS by 2.3 kcal/mol at 298 K from MP2/6-31+G(d) computations, which compares with the relative stability of 1.7 kcal/mol predicted from single-point MP2/6-31+G(d) calculations on the B3LYP geometries. Again, the approach of the incoming methyl group in the *endo* TS is found to be sterically impeded, since the distance from the axial hydrogen at the enolate Cγ atom to the hydrogen atom in the incoming methyl group is 2.263 Å (see Figure S1 in Supporting Information). These findings, therefore, support the geometrical and energetic trends derived from MP2/6-31+G(d)//B3LYP/6-31+G(d) calculations.

Finally, the potential effect of solvation on the *endo*/*exo* methyl chloride alkylation of the enolate of oxazolopiperidone **13** was examined by combining gas-phase results with solvation free energies. The most relevant effect of solvation is the stabilization of the postreaction complexes as the polarity of the solvent is increased (see Table 2), as expected from the favorable solvation of the chloride anion released upon formation of the C_α-C_M bond. In contrast, there is little influence on

Table 2. Free Energy Differences (at 298 K; kcal/mol) of Prereaction Complex (pre-RC), Transition State (TS), and Postreaction Complex (post-RC) Formed in the Reaction of the Enolate Derived from **13** with Methyl Chloride in Gas Phase and in Solution

solvent	approach	pre-RC	TS	post-RC
		MP2/6-31+G(d)		
gas phase	*exo*	0.0	11.3	−55.4
	endo	0.0	13.0	−50.5
CCl_4	*exo*	0.1	10.9	−58.6
	endo	0.0	12.5	−54.5
$CHCl_3$	*exo*	0.2	10.8	−61.5
	endo	0.0	12.2	−58.1
octanol	*exo*	0.4	10.7	−63.1
	endo	0.0	12.1	−60.2
water	*exo*	0.5	10.7	−66.8
	endo	0.0	12.0	−63.9
		MP2/aug-cc-pVDZ		
gas phase	*exo*	0.0	7.6	−56.3
	endo	0.0	9.3	−51.7
CCl_4	*exo*	0.1	7.2	−59.5
	endo	0.0	8.8	−55.7
$CHCl_3$	*exo*	0.2	7.1	−62.4
	endo	0.0	8.5	−59.3
octanol	*exo*	0.4	7.0	−64.0
	endo	0.0	8.4	−61.4
water	*exo*	0.5	7.0	−67.7
	endo	0.0	8.3	−65.1
		Best Estimate[a]		
gas phase	*exo*	0.0	8.6	−57.2
	endo	0.0	10.0	−52.7
CCl_4	*exo*	0.1	8.2	−60.4
	endo	0.0	9.5	−56.7
$CHCl_3$	*exo*	0.2	8.1	−63.3
	endo	0.0	9.2	−60.3
octanol	*exo*	0.4	8.0	−64.9
	endo	0.0	9.1	−62.4
water	*exo*	0.5	8.0	−68.6
	endo	0.0	9.0	−66.1

[a] Values determined from MP2/aug-cc-pVDZ+[CCSD-MP2/6-31+G(d)] calculations.

(27) An alternative conformation was also found for the *endo* and *exo* TS structures formed in the addition of methyl chloride to the enolate of **13**. Compared to the TSs shown in Figure 1, these alternative TSs are less stable (from computations at the MP2/6-31+G(d) level) and mainly differ in the larger planarity of the five-membered ring. In agreement with the data shown in Figure 1, the *exo* attack is favored by 1.5 kcal/mol, and the destabilization of the *endo* TS stems from the short contact between the incoming methyl group and the hydrogen atom at the gamma position in the enolate.

Table 3. Energy (Corrected for Zero-Point Energy; ZPE)[a] and Free Energy Differences (at 298 K; kcal/mol)[a] of Separated Products Formed in the Reaction of **7a** and **10a** with Methyl Chloride Relative to Separated Reactants in the Gas Phase and in Solution

	gas		CCl_4	$CHCl_3$	octanol	water
product	$\Delta(E+\text{ZPE})$	ΔG	ΔG	ΔG	ΔG	ΔG
			Compound **7a**			
8a (*exo*)	−48.3	−43.7	−49.7	−52.9	−54.7	−57.3
	−49.8	*−45.2*	*−51.2*	*−54.4*	*−56.2*	*−58.8*
9a (*endo*)	−47.5	−43.0	−49.0	−52.2	−54.1	−56.6
	−49.2	*−44.6*	*−50.6*	*−53.8*	*−55.7*	*−58.2*
Δ^b	+0.8	+0.7	+0.7	+0.7	+0.6	+0.7
	+0.6	*+0.6*	*+0.6*	*+0.6*	*+0.5*	*+0.6*
			Compound **10a**			
11a (*exo*)	−49.2	−45.3	−51.1	−54.2	−56.0	−58.1
	−50.8	*−46.9*	*−52.7*	*−55.8*	*−57.6*	*−59.7*
12a (*endo*)	−48.6	−44.8	−50.6	−53.7	−55.5	−57.6
	−50.5	*−46.6*	*−52.4*	*−55.5*	*−57.3*	*−59.4*
Δ^b	+0.6	+0.5	+0.5	+0.5	+0.5	+0.5
	+0.3	*+0.3*	*+0.3*	*+0.3*	*+0.3*	*+0.3*

[a] Values determined by subtracting the (free) energy of reactants (enolate of **7a** or **10a** and methyl chloride) from the (free) energy of products (**8a** and **9a** from **7a** or **11a** and **12a** from **10a**, and chloride anion). Values obtained from MP2/6-31+G(d) (plain) and MP2/aug-cc-pVDZ (italics) calculations are given. [b] *Endo* − *Exo*.

the activation free energy, and the stereoselectivity experimentally observed in the alkylation of **13** in tetrahydrofuran reflects the preferential stabilization of the transition state leading to the *exo* product.

In summary, the preceding results point out that the alkylation of the unsubstituted oxazolopiperidone **13** mainly affords the *exo* product **14**, which is predicted to be thermodynamically more stable than the *endo* product **15**. Indeed, alkylation through the *exo* face is favored from the differential steric hindrance experienced by the incoming alkyl group in the *endo* and *exo* faces of the enolate. These findings are in agreement with the experimental data obtained in the alkylation of bicyclic lactams **7**, but differ from those observed for **10** (see Scheme 2), thus suggesting that the phenyl substituent attached at position 3 of the oxazolopiperidone unit exerts a critical role in modulating the stereoselectivity of the process.

Effect of the Phenyl Substituent in Lactams 7 and 10. Based on the preceding considerations, it is not clear why the presence of a phenyl substituent at C3 retains the *exo* preference in the alkylation of **7** but leads preferentially to the *endo* product in **10**. This question is even more challenging when one examines the relative stabilities of the *endo* and *exo* products (see Table 3), since the latter is found to be more stable in the two compounds both in the gas phase and in solution, which suggests that the *endo*/*exo* preference might be determined by kinetic effects.

To investigate the diastereofacial selectivity in the alkylation of **7a**, we determined the TS structures for the *endo*/*exo* alkylation with methyl chloride. The TS for the *endo* approach is destabilized by 0.5 kcal/mol relative to the *exo* TS (see Figure 2), where the $C_\alpha-C_M$ distance (2.459 Å) is 0.033 Å shorter than that in the *endo* TS (2.492 Å). As noted for the unsubstituted oxazolopiperidone **13**, the more eclipsed arrangement in the *exo* TS is counterbalanced by the steric hindrance between the incoming methyl group and the axial hydrogen at the enolate $C\gamma$ atom (H···H distance of 2.322 Å) in the *endo* TS, thus explaining the destabilization of this latter TS.

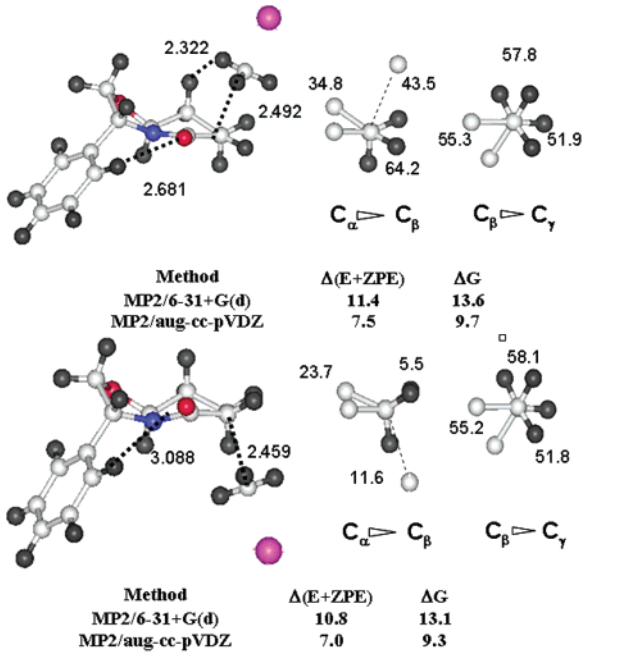

Figure 2. Transition structures for the *endo* (top) and *exo* (bottom) addition of methyl chloride to the enolate of phenyl-substituted oxazolopiperidone **7a**. Energies (corrected for zero-point energy; ZPE) and free energies (at 298 K; kcal/mol) determined at the MP2/6-31+G(d) and MP2/aug-cc-pVDZ levels relative to the most stable prereaction complex are also shown, together with the Newman projections viewed from the directions along the $C_\alpha-C_\beta$ and $C_\beta-C_\gamma$ bonds.

Though the preferential formation of the *exo* product in **7a** arises from the same factors that modulate the stereoselective alkylation in the parent compound **13**, a notheworthy feature, nevertheless, concerns the relative stability between *endo* and *exo* transition states, which is notably smaller upon attachment of the phenyl substituent (0.4 kcal/mol in **7a** versus 1.7 kcal/mol in **13**). This effect can be explained by the formation of an intramolecular C−H···O interaction between one of the phenyl $C_{ortho}-H$ hydrogens and the carbonyl oxygen in the *endo* TS (H···O distance of 2.681 Å; see Figure 2), as noted by the existence of a bond path linking the (C_{ortho})H and O atoms (ρ_{bcp} = 0.0072 au). However, such an interaction is lost in the *exo* TS (H···O distance of 3.088 Å), where no bond path was found between (C_{ortho})H and O atoms. Compared to the free enolate, where the (C_{ortho})H···O distance is 2.606 Å (ρ_{bcp} = 0.0084 au), the approach of the alkylating reagent by the *endo* face has no relevant effect on the (C_{ortho})H···O interaction. However, the approach by the *exo* face weakens such an intramolecular hydrogen bond, thus reducing the difference in stability between *endo* and *exo* TSs. It can, therefore, be concluded that the phenyl ring contributes to modulating the stability of the TSs in the alkylation reaction of **7**.

The TSs for the alkylation reaction of **10a** in the gas phase are shown in Figure 3. In contrast to the results obtained for **13** and **7a**, the $C_\alpha-C_M$ distance in the *endo* TS (2.481 Å) is around 0.01 Å shorter than that in the *exo* TS (2.489 Å), which is now destabilized by 0.8 kcal/mol with regard to the *endo* TS. Indeed, there is not a specific interaction leading to the steric destabilization of one of the two TSs, since the closest interatomic distances between the incoming methyl group and the enolate (2.533 Å with the equatorial hydrogen in C_β for *endo* TS; 2.477 Å with the hydrogen bonded at the angular carbon for *exo* TS)

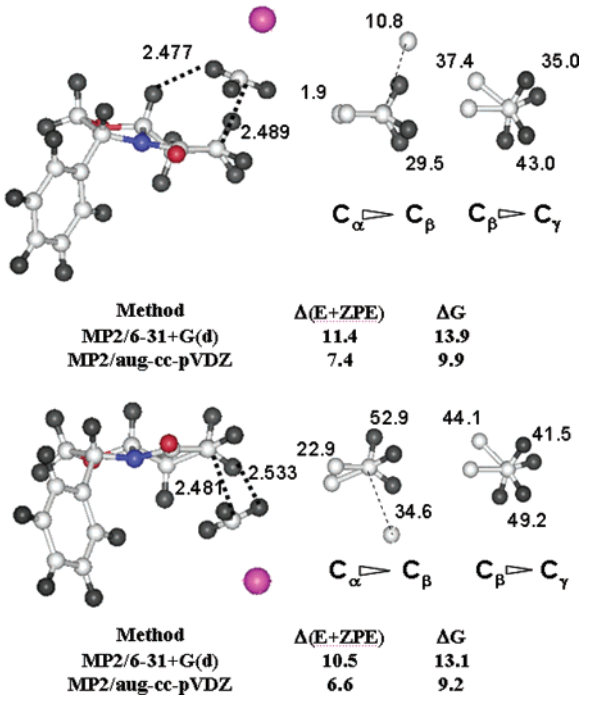

Figure 3. Transition structures for the *exo* (top) and *endo* (bottom) addition of methyl chloride to the enolate of phenyl-substituted oxazolopiperidone **10a**. Energies (corrected for zero-point energy; ZPE) and free energies (at 298 K; kcal/mol) determined at the MP2/6-31+G(d) and MP2/aug-cc-pVDZ levels relative to the most stable prereaction complex are also shown, together with the Newman projections viewed from the directions along the $C_\alpha-C_\beta$ and $C_\beta-C_\gamma$ bonds.

are larger than the sum of van der Waals radii. Therefore, the destabilization of the *exo* TS can be mainly attributed to the torsional strain induced by the approach of the incoming methyl group, which forces the enolate to adopt an eclipsed arrangement along the $C_\alpha-C_\beta$ bond, whereas the *endo* approach occurs through a more staggered conformation (see Newman projections in Figure 3).

As noted above for the alkylation of the enolate of oxazolopiperidone **13**, the postreaction complexes formed from **7a** and **10a** are largely stabilized as the polarity of the solvent increases (see Table 4), this effect being slightly larger for the *exo* addition. However, it does not change the general trends of the energy profile determined in the gas phase, and the *endo*/*exo* preference is mainly guided by the intrinsic gas-phase effects related to the differential stability of the corresponding TSs, which is controlled by two different factors. In the enolate derived from **7a**, though the approach by the *exo* face leads to a more eclipsed conformation in the enolate, the destabilization of the *endo* TS arises from the steric hindrance between the alkylating group and the axial hydrogen at the Cγ position. However, in the enolate derived from **10a**, the *endo*/*exo* preference is mainly dictated by the torsional strain induced in the enolate upon approach of the alkylating reagent.

Influence of Li^+ Coordination on the Stereoselective Alkylation of the Oxazolopiperidone Enolate. Recent studies have suggested that coordination with a Li^+ cation may be responsible for the stereochemical outcome in Meyers-type enolate alkylations.[7] In fact, the hypothesis that the diastereofacial selectivity observed in these reactions might result from specific interactions with a solvated Li^+ cation was already proposed in 1990.[28] Nevertheless, the potential influence exerted by solvation and Li^+ coordination was not supported by a series of experimental results reported by Romo and Meyers,[2a] who stated that "*it would appear that neither the aggregation state of the enolate nor the coordination sphere about lithium plays a major role in the observed selectivity*." These findings received further support from the theoretical studies recently reported by Ando,[9] who carried out a detailed analysis of the potential influence of solvated Li^+ cation on the stereoselective alkylation of enolates of γ-butyrolactones. The results were conclusive in showing that complexation with Li^+ had a negligible effect on the relative stability of the transition states leading to *exo* and *endo* addition. Since the stereochemical outcome in the alkylation of γ-butyrolactones is determined by the different torsional strain in the *endo* and *exo* TSs, it is reasonable to expect that

Table 4. Free Energy Differences[a] (at 298 K; kcal/mol) of Prereaction Complex (pre-RC), Transition State (TS), and Postreaction Complex (post-RC) in Solution Formed in the Reaction of the Enolates Derived from **7a** and **10a** with Methyl Chloride

solvent	approach	pre-RC	TS	post-RC
		Compound **7a**		
gas phase	*exo*	0.0	13.1	−50.8
		0.0	*9.3*	*−51.9*
	endo	0.5	13.6	−50.7
		0.4	*9.7*	*−52.1*
CCl_4	*exo*	0.0	12.2	−54.9
		0.0	*8.4*	*−56.0*
	endo	0.7	12.9	−54.3
		0.6	*9.0*	*−55.7*
$CHCl_3$	*exo*	0.0	11.6	−58.6
		0.0	*7.8*	*−59.7*
	endo	0.9	12.3	−57.5
		0.8	*8.4*	*−58.9*
octanol	*exo*	0.0	11.3	−60.7
		0.0	*7.5*	*−61.8*
	endo	1.2	11.9	−59.6
		1.1	*8.0*	*−61.0*
water	*exo*	0.0	11.8	−63.6
		0.0	*8.0*	*−64.7*
	endo	1.3	12.7	−61.7
		1.2	*8.8*	*−63.1*
		Compound **10a**		
gas phase	*exo*	0.5	13.9	−53.7
		0.5	*9.9*	*−54.5*
	endo	0.0	13.1	−50.8
		0.0	*9.2*	*−52.8*
CCl_4	*exo*	0.5	12.8	−57.4
		0.5	*8.8*	*−58.2*
	endo	0.0	12.0	−54.3
		0.0	*8.1*	*−56.3*
$CHCl_3$	*exo*	0.5	12.0	−60.6
		0.5	*8.0*	*−61.4*
	endo	0.0	11.2	−57.6
		0.0	*7.3*	*−59.6*
octanol	*exo*	0.4	11.4	−62.3
		0.4	*7.4*	*−63.1*
	endo	0.0	10.8	−59.5
		0.0	*6.9*	*−61.5*
water	*exo*	0.3	12.1	−64.4
		0.3	*8.1*	*−65.2*
	endo	0.0	11.5	−62.5
		0.0	*7.6*	*−64.5*

[a] Values determined from MP2/6-31+G(d) (plain) and MP2/aug-cc-pVDZ (italics) calculations.

(28) Durkin, K. A.; Liotta, D. *J. Am. Chem. Soc.* **1990**, *112*, 8162.

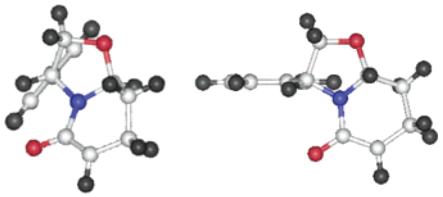

Figure 4. Top view of the enolate of phenyl-substituted oxazolopiperidone **7a** (left) and **10a** (right) in the transition structures for addition of methyl chloride (taken from the *exo* TS in **7a** and from the *endo* TS in **10a**).

coordination of the solvated Li^+ cation to the enolate of **10** will not affect the stereochemical outcome, because the diastereofacial selectivity is also governed by similar torsional strain effects (see above). However, since the alkylation in the enolate of **7** (and **13**) is predicted to be determined by the steric hindrance between the enolate and the incoming alkylating reagent (see above), it is not clear whether complexation with a solvated Li^+ cation might affect the relative stability of the two TSs.

To analyze the potential influence of the Li^+ coordination to the enolate, the TSs corresponding to the addition of methyl chloride to the enolate of **13** coordinated to a Li^+ cation solvated by two THF molecules were determined at the B3LYP/6-31+G(d) level (the optimized structures are shown in Figure S2 in Supporting Information). Compared to the results shown in Figure 1, the length of the forming $C_\alpha-C_M$ bonds in the two TSs are shortened by around 0.14 Å. Nevertheless, the $C_\alpha-C_M$ bond length in the *exo* TS (2.371 Å) is 0.021 Å shorter than that in the *endo* TS (2.350 Å), which agrees with the geometrical difference found from B3LYP/6-31+G(d) geometry optimizations for the attack of methyl chloride to the enolate of **13** (0.031 Å; see Figure 1). Moreover, the intermolecular H···H distance between the hydrogen atoms bonded at the enolate Cγ atom and the incoming methyl group amounts to 2.392 Å, which compares with the H···H distance of 2.339 Å found in the absence of the solvated Li^+ cation (see Figure 1). Finally, the *endo* TS is destabilized by 1.2 kcal/mol at 298 K relative to the *exo* TS, which compares with the 1.7 kcal/mol destabilization reported in Figure 1, and the relative stability of the two TS was indeed little affected upon addition of the free energies of solvation determined from MST calculations in carbon tetrachloride, chloroform, octanol, and water. Therefore, these findings suggest that coordination of a solvated Li^+ cation to the enolate does not play a crucial role in modulating the stereochemical outcome of the reaction.

What Controls the Diastereoselective Alkylation in the Enolates derived from 7 and 10? In the enolate derived from **10a**, the phenyl ring is oriented so that one of the *ortho* carbon atoms adopts a *syn* arrangement relative to the nitrogen atom (C_{ortho}-C$-C_3-$N torsion of $-32.4°$ and $-36.1°$ in *endo* and *exo* TSs, respectively; see Figure 4). In this arrangement the bicyclic system is roughly planar, and the *endo*/*exo* preference is mainly dictated by the torsional strain induced in the enolate upon approach of the alkylating reagent. The stereoselectivity in the alkylation is, therefore, governed by factors similar to those identified in the alkylation of enolates in related five-membered ring lactams[8] and lactones.[9] In compound **7a**, nevertheless, the configuration of the angular carbon impedes the phenyl ring to protrude into the *endo* face. Accordingly, this lactam must adopt a different conformation characterized by a $C_{ortho}-C-C-N$ torsional angle of 84.6° and 87.5° in *endo* and *exo* TSs, respectively (see Figure 4). In this conformation the bicyclic system deviates from a planar arrangement, as also found in the unsubstituted oxazolopiperidone **13** (see above), and the accessibility through the *endo* and *exo* faces to an incoming alkylating reagent is no longer equivalent. Thus, though the approach by the *exo* face leads to a more eclipsed conformation in the enolate, the destabilization of the *endo* TS arises from the steric hindrance between the alkylating group and the axial hydrogen at the Cγ position.

The results obtained for oxazolopiperidones **13** and **7a** indicate that the preferred alkylation path (i.e., the *exo* addition) corresponds to the TS that exhibits the largest internal torsional strain, because the stereoselectivity is controlled by the larger steric hindrance between the enolate and the alkylating reagent in the *endo* transition state. The role played by steric effects in determining the stereochemical outcome was also pointed out by Houk and co-workers in their studies performed for the addition of methyl chloride to a bicyclic pyrrolidinone lactam.[8] However, whereas in this latter case the steric hindrance comes from the contact between the incoming methyl group and the fused oxazolidine ring (see Figure 2 in ref 8), the steric hindrance in the alkylation of **13** and **7a** comes from the contact between the incoming methyl group and the carbon atom at the γ position relative to the carbonyl group. In other words, while in [3.3.0] lactams the steric hindrance in the alkylation reaction involves the adjacent ring, in [4.3.0] lactams it comes precisely from the ring that undergoes the alkylation. This is a consequence of the less flexible, more crowded nature of [3.3.0] systems compared to [4.3.0] systems and clearly indicates that the origin of the stereoselecvity, though determined by steric effects in both cases, is completely different.

The results presented here explain why reversion of the chirality of the angular carbon leads to a complete change in the stereoselectivity of the alkylation of compounds **7** and **10**. This can be realized by the fact that the alkylation is governed by intramolecular torsional strain of the enolate in one case (**10**) but by the intermolecular hindrance between the enolate and the alkylating agent in the other (**7**). Indeed, such a change is critically dependent on the orientation adopted by the phenyl group attached at position 3, thus revealing a completely unexpected role for a substituent that is *apparently apart* from the alkylation position.

Finally, the results also provide clues to designing chemical modifications to alter the facial stereoselectivity in **7**. This synthetic approach would take advantage of the intramolecular hydrogen bond formed between the phenyl ring and the carbonyl oxygen in the enolate of **7**, which largely reduces the difference in stability of the two transition states compared to the unsubstituted oxazolopiperidone. Therefore, it is reasonable to expect that strengthening such a hydrogen bond (for instance, through the introduction of adequate electron-withdrawing substituents on the phenyl ring) might further destabilize the *exo* TS and eventually modify the stereoselectivity of the alkylation. These findings, therefore, can open the way to designing molecular mechanisms that might be used to modulate the diastereoselective alkylation in substituted oxazolopiperidones.

Conclusions

The differences observed experimentally in the diastereoselective alkylation of the phenyl-substituted oxazolopiperidones

7 and **10** can be rationalized from the delicate balance between several effects, whose magnitude can ultimately be ascribed to the influence exerted by the phenyl substituent at position 3. When the angular carbon adopts an *R* configuration (**10**), the phenyl ring forces the *pseudo*-planarity of the bicyclic lactam and the diastereoselectivity is dictated by the internal torsional strain induced in the enolate. However, when the angular carbon adopts an *S* configuration (**7**), the preference for the *exo* alkylation is dictated by the intermolecular steric hindrance between the enolate and the alkylating reagent, although the origin of this steric hindrance is different from that of five-membered [3.3.0] lactams.

Acknowledgment. We are grateful to Prof. J. Tomasi for providing us with his original code of the PCM model, which was modified by us to carry out the MST calculations. I. Barcena is acknowledged for her technical assistance. This work was supported by the Spanish Ministry of Science and Technology-FEDER (SAF2002-04282 and BQU2003-00505), and the Centre de Supercomputació de Catalunya. Thanks are also due to the DURSI, Generalitat de Catalunya, for Grant 2005SGR-0603 and to the Ministry of Education and Science for fellowships to I.S. and O.L.

Supporting Information Available: Complete ref 22, graphical representation of the transition states for the attack of methyl chloride to the enolate of **13** (MP2/6-31+G(d) level) and to the enolate coordinated to $Li^+(THF)_2$ (B3LYP/6-31+G(d) level), and the B3LYP/6-31+G(d) geometries and energies of the separated reactants and products as well as of the stationary points for the reaction of enolates derived from **13**, **7**, and **10** with methyl chloride. This material is available free of charge via the Internet at http://pubs.acs.org.

JA055393M